Int J Clin Exp Med 2015;8(6):8398-8414
www.ijcem.com /ISSN:1940-5901/IJCEM0008907

Original Article

The preparation of core/shell structured microsphere of multi first-line anti-tuberculosis drugs and evaluation of biological safety

Hao Zeng[1], Xiaoyang Pang[2], Shuo Wang[3], Zhengquan Xu[1], Wei Peng[1], Penghui Zhang[1], Yupeng Zhang[1], Zheng Liu[1], Chengke Luo[1], Xiyang Wang[1], Hemin Nie[3]

[1]Department of Spine Surgery, The Xiangya Hospital of Central South University, 87# Xiangya Road, Changsha 410008, People's Republic of China; [2]Department of Orthopedics Surgery, The Xiangya Hospital of Central South University, 87# Xiangya Road, Changsha 410008, People's Republic of China; [3]Department of Biomedical Engineering, College of Biology, Hunan University, Changsha 410082, People's Republic of China

Received April 8, 2015; Accepted June 7, 2015; Epub June 15, 2015; Published June 30, 2015

Abstract: To introduce a modified method, namely coaxial electrohydrodynamic atomization for the fabrication of distinct core/shell structured microspheres of four first-line ant-tuberculosis drugs with different characteristics in hydrophilic properties in one single step. In group B, we prepared microspheres in which the core and the shell contain hydrophobic and hydrophilic drugs, respectively. In contrast, in group C, the opposite is prepared. The detection of encapsulation efficiency and in vitro release test were performed to confirm the feasibility of the drug-loaded core/shell structured microspheres. Moreover, cell culture experiments and animal experiments have been carried out to evaluate the biological safety of different microspheres in cell growth, cell viability, osteogenesis and migration of BMSCs in vitro and the bone fusion in a bone deficits model in SD rat. Meanwhile, the distribution of drugs and liver and kidney toxicity were monitored. The release patterns of the two groups are significantly different. The release of drugs from Group B microspheres is rather sequential, whereas group C microspheres release drugs in a parallel (co-release) manner. And various concentrations of carrier materials produces core/shell structured microspheres with different appearance. Moreover, the biological safety of core/shell structured microspheres was testified to be satisfactory. These findings present the advantages and possible application of this kind of multi-drug release system in treating skeletal tuberculosis. Moreover, the characteristic sequential release of multi-drugs can be controlled and adjusted based on treatment need and used in treating other disorders.

Keywords: Core/shell structure, microspheres, multi drugs, co-release, ant-tuberculosis drugs

Introduction

Tuberculosis (TB) remains a growing public health problem especially in developing countries. The epidemiology of TB is driven by the natural history of the disease and the susceptibility of the at-risk population. About one-third of the world's population has been infected with TB and has latent tuberculosis infection [1, 2]. Bone and joint tuberculosis is recognized as the highest incidence of extra-pulmonary tuberculosis, accounting for 35-50% of extra-pulmonary, and 3-5% of the total TB tuberculosis [3, 4].

Ant-TB chemotherapy is the key to the treatment of tuberculosis, but the conventional oral administrations were characterized as low blood concentrations and even lower local concentration in lesions, which easily result in drug resistance to tuberculosis and recurrence [5]. Moreover, long-term and systemic administration of anti-TB drugs easily leads to severe complications, such as liver and kidney toxicity and neurotoxicity. The topical application of TB drugs can effectively increase the local concentration of TB drugs and theoretically reduce drug side effects [6].

Chemotherapy through local drug delivery using biodegradable polymeric materials showed promise [5]. However, most current biodegradable delivery systems deal with the delivery of one single anti-TB agent, which is not practica-

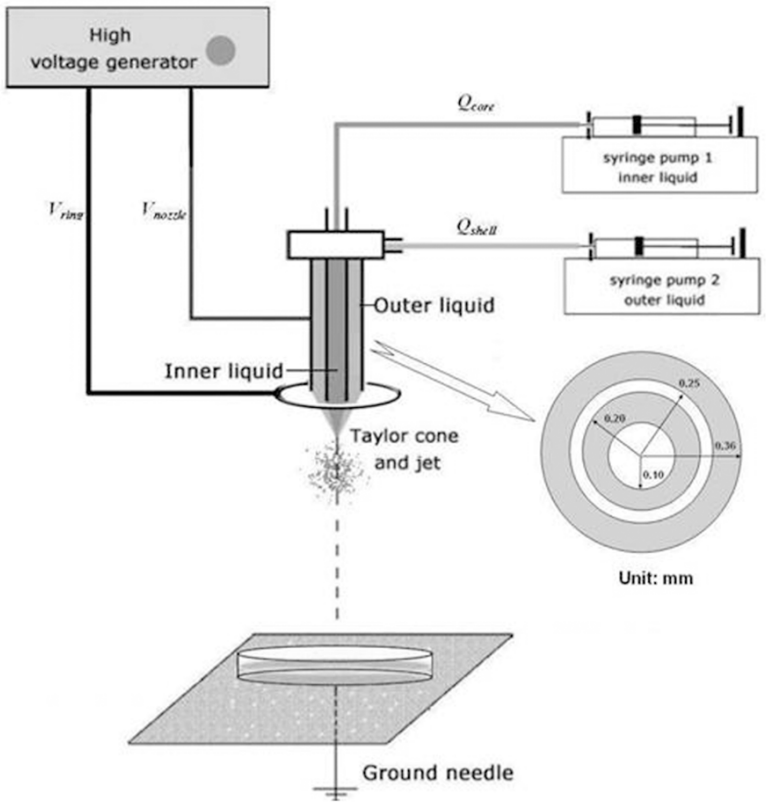

Figure 1. The schematic diagram of coaxial electrohydrodynamic atomization device (CEHDA). V_{ring} and V_{nozzle} are 3.5 KV and 6.5 KV, the flow rate ratio (Q_{core}/Q_{shell}) are 1.5 mL/h/2.0 mL/h respectively, in a typical fabrication.

ble for tuberculosis therapy in most cases [7]. Anti-TB treatment is a multi-factor process that is modulated by a serial of regulatory factors, such as drug types and quantity, frequency and time of administration and patients' health and compliance [8]. As each drug exhibits a distinct time-dependent concentration profile during the inhibition or sterilization process, sequential or coupled release of multiple drugs with specific temporal profiles is expected to be critical to the successful curing tuberculosis. The present study will use the coaxial electrohydrodynamic atomization (CEHDA) equipment to fabricate the core/shell structured microsphere of four first-line anti-TB drugs and comprehensively investigate their biological safety in vitro and in vivo.

Materials and methods

The investigation conforms to the Guide for the Care and Use of Laboratory Animals published by the US National Institutes of Health (NIH Publication No. 85-23, revised 1996). The study protocol was approved by the Xiangya Hospital Ethics Committee.

Materials and experimental set-up

Poly-L-lactide (PLLA, M_W = 85,000-160,000), poly (D, L-lactide-co-glycolide) copolymer with lactide/glycolide molar ratio of 50:50 (PLGA, M_W = 40,000-75,000), rifampicin, pyrazinamide isoniazid and ethambutol hydrochloride were harvested from Sigma-Aldrich (St. Louis, MO). Dichloromethane (DCM), anhydrous ethanol and ethyl acetate (EA) were all acquired from Kermel Chemical Reagent Co. Ltd (Tianjin, China). Coumarin-6, dialysis bag, phosphate buffer saline (PBS), fetal bovine serum (FBS) and commercial Spectro/Por membrane (molecular weight cut-off: 3500) were purchased from Bai Sai Biological Technology Co. Ltd (Shanghai, China), Blue Reagent Factory (Shanghai, China), Yuanye Biological Technology Co. Ltd (Shanghai, China), Xinfan Biological Technology Co. Ltd (Shanghai, China) and Spectrum Laboratories (Rancho Dominguez, CA), respectively.

Coaxial needle (Popper and Sons, Lake Success, NY) is manufactured of 316L stainless steel. The core capillary presents a 0.40 mm outer diameter and a 0.20 mm inner diameter and the outer capillary has a 0.72 mm in outer diameter and a 0.50 mm in inner diameter. Two syringe pumps (KD Scientific, Holliston, MA) deliver the polymer solution at a specific rate into the outer and inner capillary of coaxial needle. A voltage generator (Glassman High Voltage, High Bridge, NJ) supplies a high voltage to the nozzle by a crocodile clip. To stabilize the electric field surrounding the nozzle, the other high voltage (Glassman High Voltage, High Bridge, NJ) is used to the ring (5 cm in

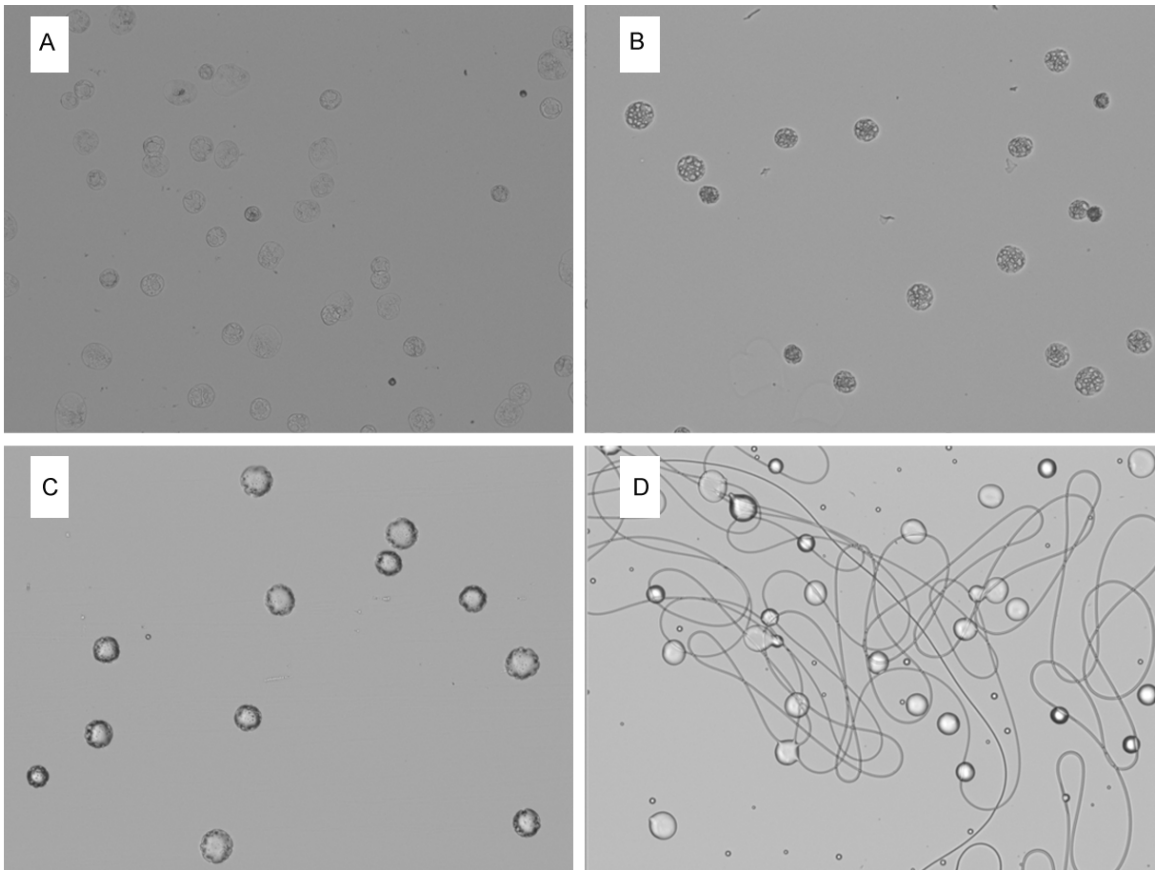

Figure 2. Results of different carrier concentration under ordinary light microscope. (A-D) represents the concentration of PLLA and PLGA of 5%, 7.5%, 10% and 12.5%.

diameter) around a nozzle (**Figure 1**). By increasing the ring voltage (V_{ring}) and nozzle voltage (V_{nozzle}), the newly-presented drops were gradually accelerated via the potential difference until a stable Taylor cone jet can be obviously observed. In order to avoid microsphere agglomeration, a petri dish filled with anhydrous ethanol was provided to collect the microspheres, replacing the normal aluminum foil.

Microsphere fabrication

Concentration of PLGA and PLLA for microsphere fabrication: The objective is to fabricate, by CEHDA, microspheres of distinct core/shell structures. To ensure that the drug in the core is not released prematurely, the core must be of slower degrading material than the shell. Hence, PLLA was chosen for the core and PLGA for the shell in this study. PLLA was dissolved with DCM and PLGA was dissolved using EA. The concentration of PLLA and PLGA was prepared with 5%, 7.5%, 10% and 12.5%, respectively. PLLA was added a trace of coumarin-6. PLLA was transmitted by pump 1, PLGA solution by pump 2. The flow rates of pump 1 and 2 flow are set to 1.5 ml/h. The velocity of flowing droplet in coaxial needlepoint stabilized well, followed by turned on voltage (V_{ring} = 3.5 KV, V_{nozzle} = 6.5 KV) (**Figure 1**). After the Taylor cone jet stabilized, we used a petri dish with anhydrous ethanol to collect microspheres. During the process of spraying, we used a slides glass in a spray area to collect a small amount of microspheres in each group for detecting the microsphere size with ordinary light microscope (OLM) and confocal laser scanning microscopy (CLSM). Microspheres were centrifuged, washed by PBS repeatedly three times, freeze-dried for 48 h and the frozen microspheres were performed by the scanning electron microscopy (SEM) detection.

The preparation of core/shell structure microsphere of four first-line anti-tuberculosis drugs

Ideally, rifampicin/pyrazinamide (RFP/PZA) and isoniazid/ethambutol hydrochloride (INH/

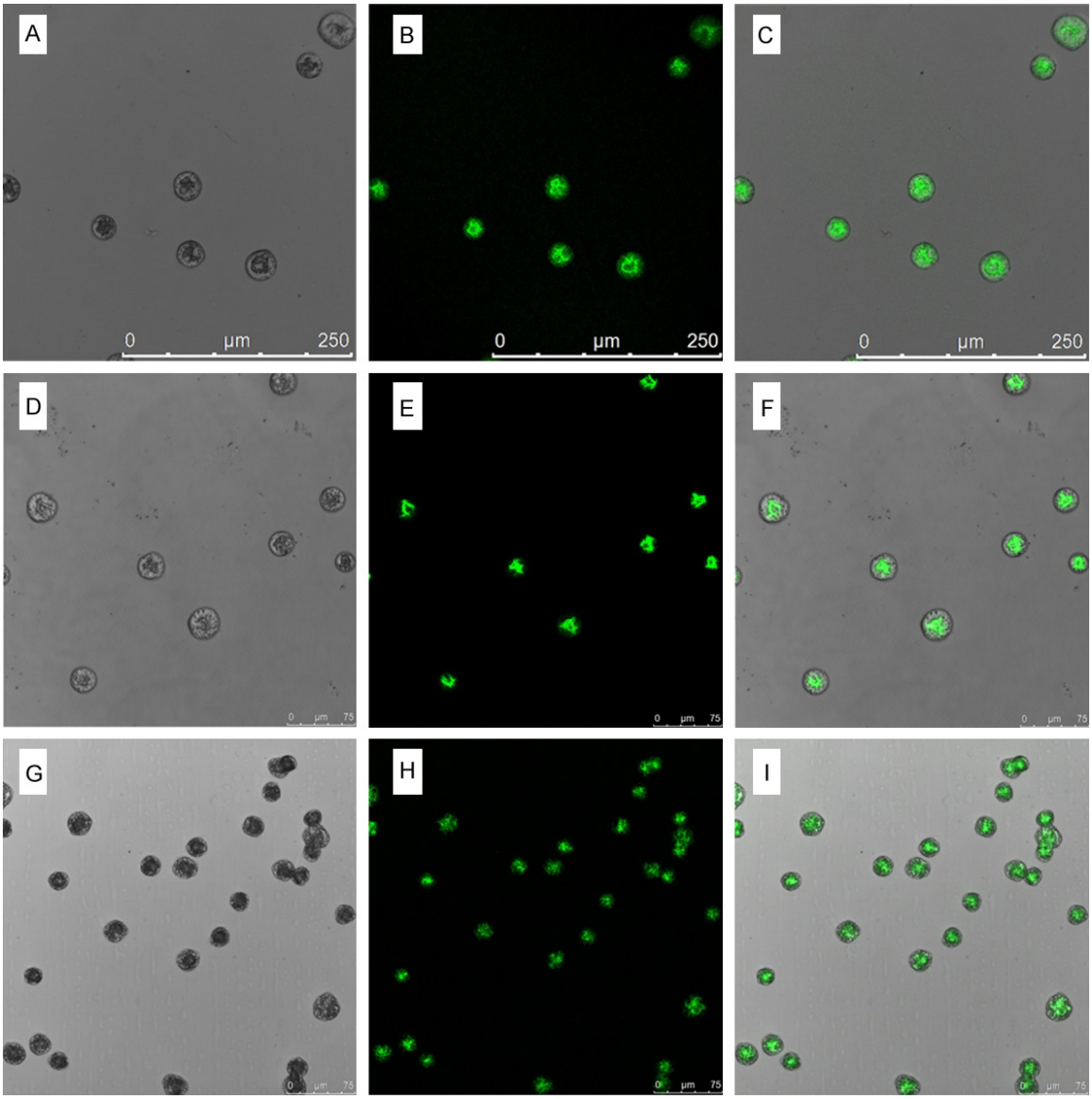

Figure 3. Results of different carrier concentration under confocal laser scanning microscopy (CLSM). (A-C, D-F, G-I) represents the concentration of PLLA and PLGA of 5%, 7.5% and 10%, respectively. PLLA added within coumarin-6 manifests green in the excitation blue light of CLSM, which is only confined to the core structure, while the shell is not rendered. When the same fields of view image under ordinary light microscope (A, D, G) and CLSM (B, E, H, respectively) are superimposed for synthesis (C, F, I respectively), it can be determined whether the microspheres have the core/shell structure or not.

EMBH) are encapsulated in PLLA core and PLGA shell (the optimum concentration of PLLA and PLGA is confirmed 10% in the context), respectively, or the reverse in radial distribution, with INH/EMBH inside the core and RFP/PZA in the shell. Therefore, the release of four drugs can be predicted and controlled. For the former case, RFP/PZA was dissolved in PLLA/DCM solution (inner phase). As INH/EMBH sodium salt cannot be dissolved in PLGA/EA solution directly, INH/EMBH was dissolved in 95% ethanol first, before it was loaded into the shell phase (PLGA/EA). In a typical fabrication, two separate solutions of 500 mg of PLLA in 10 mL of DCM and 500 mg of PLGA in 10 mL of EA were prepared. Specifically, RFP/PZA was dissolved in PLLA/DCM solution to form a homogenous phase for the core liquid (RFP/PZA/PLLA, 2% w/w), whereas INH/EMBH sodium salt was dissolved in 95% ethanol and transferred into PLGA/EA solution for the shell liquid (INH/EMBH/PLGA, 2% w/w). For the latter case, RFP/PZA was dissolved in PLGA/EA for shell phase. Meanwhile, INH/EMBH was dissolved in

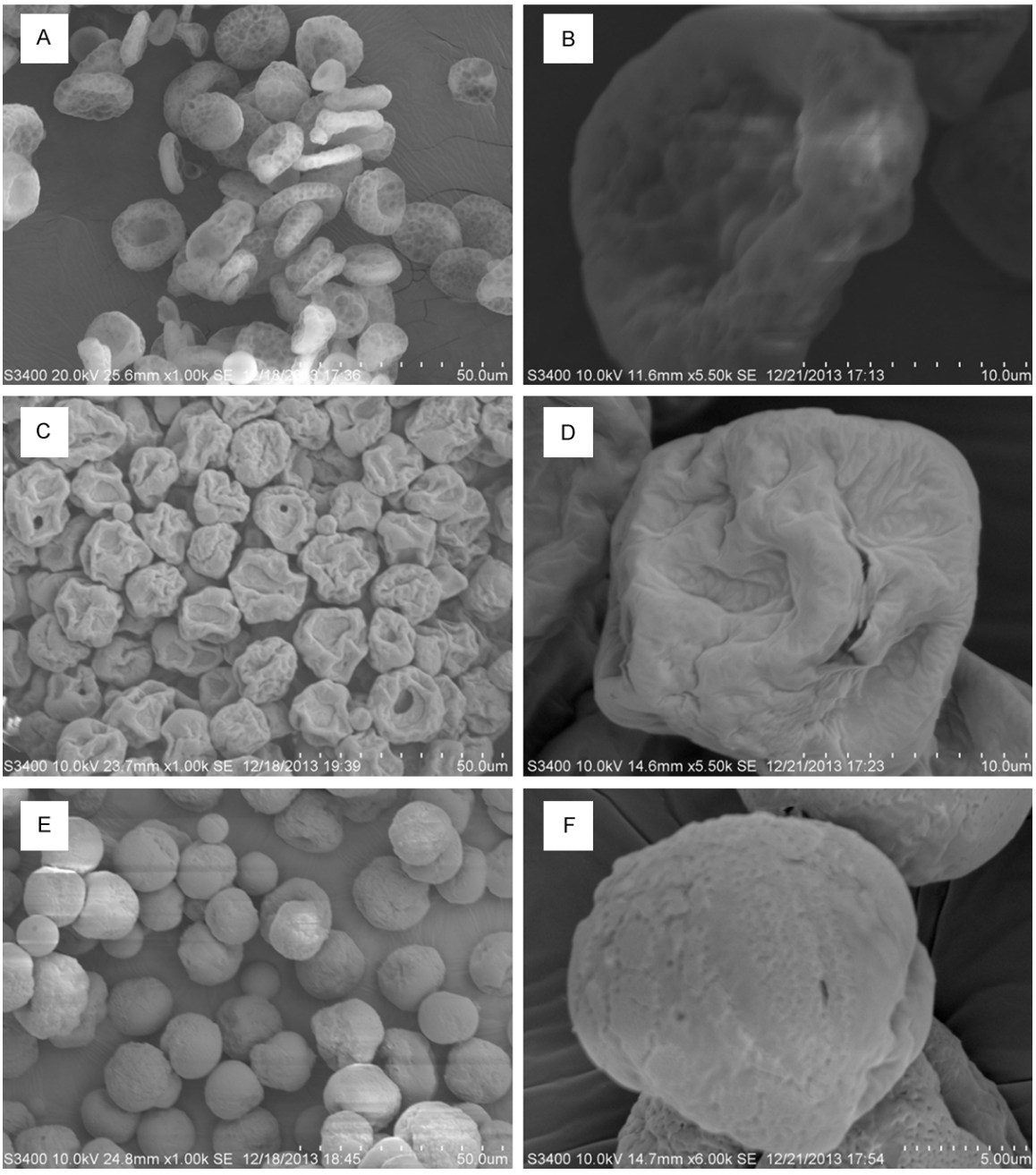

Figure 4. Results of different carrier concentration under scanning electron microscope (SEM). A, B. The microspheres with carrier concentration of 5%, showed caky, random-shaped and lacunose surface; C, D. The microsphere with carrier concentration of 7.5% presented some wrinkle but little lacuna surface; E, F. The microsphere with carrier concentration of 10%, demonstrated a smooth and stereoscopic uniformity surface without significant lacuna.

deionized water (DI) and then mixed with PLLA/DCM solution by mild ultrasonic. For both cases, the CEHDA operating parameters are around 3.5 KV for the ring and 6.5 KV for the nozzle, and the flow rates for inner phase and outer phase are 1.5 mL/h. The microspheres collected in anhydrous ethanol were centrifuged and the resultant pallets were dried in a freeze drier

Microsphere characterization

The size and general morphology of fabricated microspheres were observed by SEM. CLSM

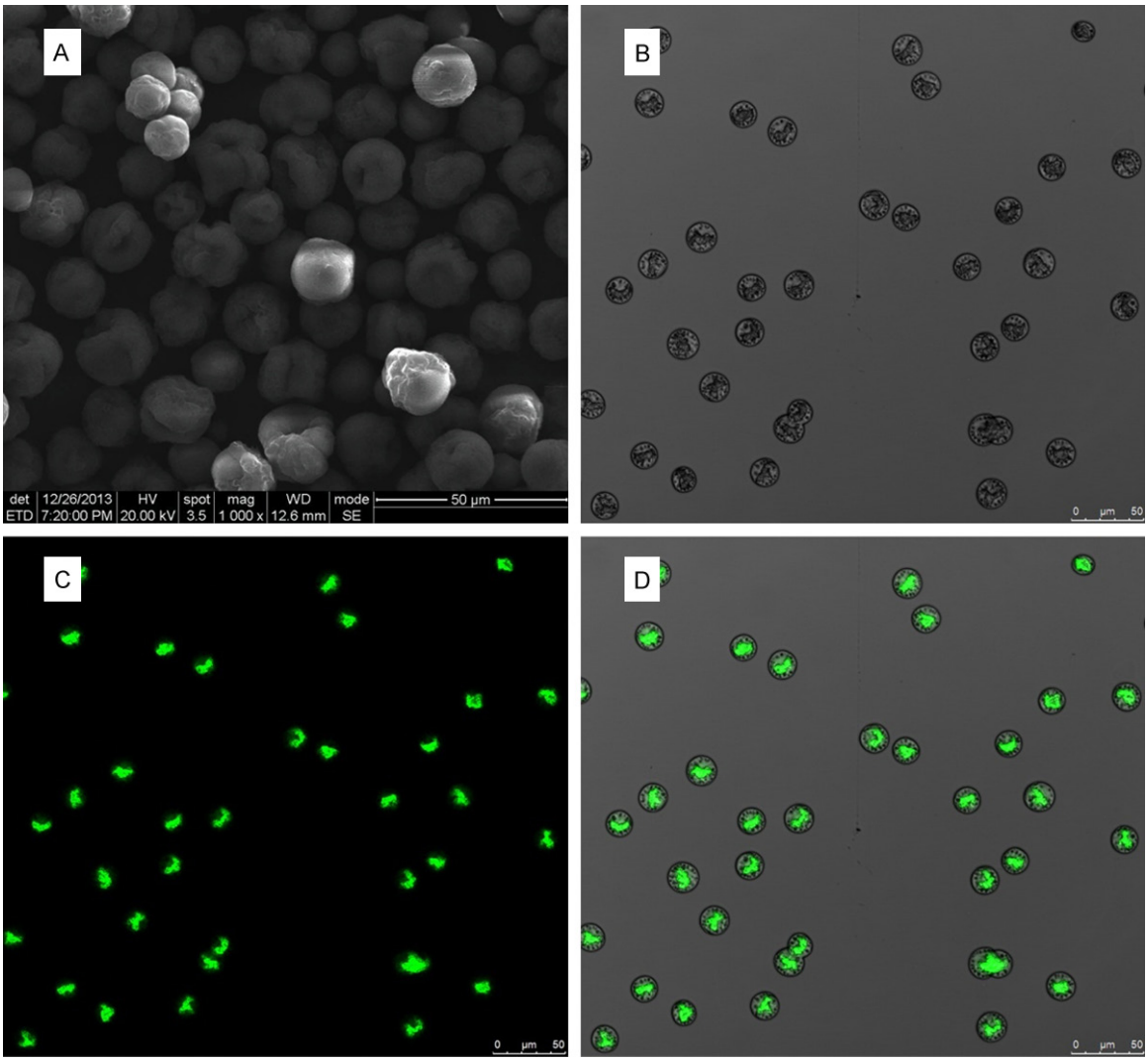

Figure 5. Confirmation of drug-loaded core/shell structures. Typical micrograph of core/shell structured microspheres (A) and confocal fluorescence images of core/shell structured microspheres with coumarin-6 stained cores (B-D). (B, C) Images collected in bright field and FITC channel respectively. (D) Overlay of figures collected in both bright field and FITC channel.

was used to observe the distribution of coumarin-6 in microspheres. The resulting distribution of dye in the microsphere can be regarded as an indicator of the extent of mixing of the inner and outer flows at the tip of the coaxial needle (**Figures 2**-**5**; **Table 1**).

Encapsulation efficiency and in vitro release of drugs

To determine the encapsulation efficiency (EE) of RFP/PZA and INH/EMBH in microspheres, 20.0 mg of RFP/PZA and INH/EMBH-loaded microspheres was dissolved in 1.0 mL DCM, and subsequently, 1.0 mL phosphate buffer solution (PBS) was introduced, vortexed, and centrifuged at 14,000 rpm for 3 min. The aqueous layer was collected, and two more extraction cycles were performed to maximize INH/EMBH recovery. The INH/EMBH concentration in aqueous phase and the RFP/PZA concentration in oil phase were both determined by a liquid chromatography electrospray ionization tandem mass spectrometry (LC-MS/MS). For in vitro release testing, 20.0 mg of RFP/PZA and INH/EMBH-loaded microspheres was loaded in a Spectro/Por membrane bag and subsequently stored the bag in a centrifuge tube with 20.0 mL of PBS (pH 7.4) containing 0.05% of Tween 80. The whole system was then placed in an orbital shaker bath maintained at 37°C and

Table 1. Statistical analysis of the diameters of microsphere in group A, B, and C

	t test						
	T value	df	Sig (bilateral)	Mean difference	Standard deviation	95% confidence interval	
						Lower limit	Upper limit
A, B	-0.176	198	0.861	-0.02500	0.14210	-0.30523	0.25523
A, C	-0.688	198	0.492	-0.10200	0.14815	-0.39416	0.19016
B, C	-0.638	198	0.524	-0.7700	0.12065	-0.31492	0.16092

Table 2. Methods of solvent configuration in each group

Groups		Methods
Group A	Core	10% PLLA + 0.4 ml DI emulsification
	Shell	10% PLGA
Group B	Core (hydrophobic)	10% PLLA (10 mL) + 50 mg RFP + 50 mg PZA)
	Shell (hydrophilic)	10% PLGA (10 mL + 0.4 ml DI + 50 mg INH + 50 mg EMBH emulsification
Group C	Core (hydrophilic)	10% PLLA (10 mL) + (0.4 ml DI + 50 mg INH + 50 mg EMBH) emulsification
	Shell (hydrophobic)	10% PLGA (10 mL) + (50 mg RFP + 50 mg PZA)

Note: DI, deionized water; RFP, rifampicin; PZA, pyrazinamide; INH, isoniazid; EMBH, ethambutol hydrochloride.

120 RPM. At given time intervals, 1.0 mL of the incubated medium was withdrawn and replaced by 1.0 mL fresh medium. RFP in the resultant release medium was first extracted with 1 mL of DCM. A mixture of acetonitrile and water (50:50 v/v) was added to the extracted RFP after the DCM had fully evaporated. Similar to EE testing, the concentrations of RFP, PZA, INH and EMBH were both determined by LC-MS/MS.

The impact of drug-loaded microspheres on biological behavior of BMSCs from SD rats

BMSCs obtained from the tibia of three male SD rats (250-300 g) were subcultured to P3 generation, and then were performed by cell cycle detection and identification of surface antigens, osteogenesis and lipogenesis (the specific process and data not shown). We evaluated the impact of microspheres on cell growth, cell viability, osteogenesis and migration of BMSCs in the blank control group, blank microspheres and drug-loaded microspheres group (INH/EMBH in core and RFP/PZA in shell, which was confirmed to be able to reach the synchronous release in the context).

Cell growth: The bone marrow mesenchymal stem cells (BMSCs) of P3 generation after being digested into a single cell suspension by the trypsin were seeded in 96-well culture plates at a concentration of 5.0×10^4 cells/well. Each well was added with 500 μL cell suspension and cultured 9 days. The blank control group was added with 5 ml DMEM of 10% fetal bovine serum (FBS) and 2% PBS; blank microspheres group was added with 5 ml DMEM of 10% FBS and 5 mg blank microspheres; drug-loaded microspheres group was joined with 5 ml DMEM of 10% FBS and 5 mg drug-loaded microspheres, each group included three parallels. Three wells culture fluid was aspirated at per 24 hours. The average value of derived cells was regarded as the cell number of the day and plotted the growth curve of BMSCs.

Cell viability: Determination of the effect of biological activity of drug-loaded microspheres on the growth of the BMSCs was identified by methyl-thiazolyl-tetrazolium (MTT) assay. The process of gaining the subjects was similar to the mentioned-above methods, but two samples in every group were performed by MTT assay to record the optical density (OD) at 490 nm wavelength after days 3, 6, 9. The detailed steps of MTT assay could refer to Qi, B., et al [9]

Osteogenesis: The BMSCs were seeded in 96-well culture plates at a concentration of 2.0×10^4 cells/cm^2. Each culture plate was added with 10 ml osteogenic liquid. The blank control group was added with 5 ml DMEM with 10% FBS; blank microspheres group was added with 5 mg blank microspheres; drug-loaded microspheres group was joined with 5 mg drug-loaded microspheres, each group included three parallels. After the replacement of the same

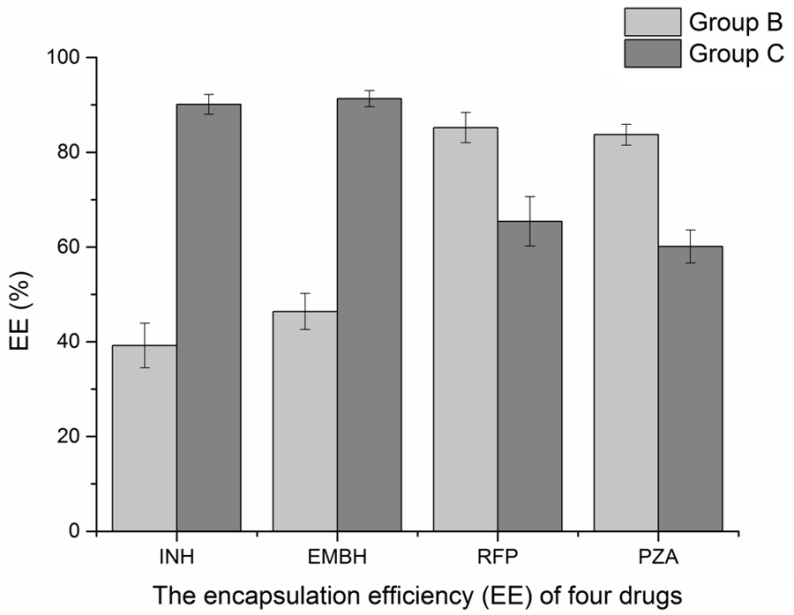

Figure 6. The encapsulation efficiency of four drugs in microspheres. INH, isoniazid; EMBH, ethambutol hydrochloride; RFP, rifampicin; PZA, pyrazinamide

liquid twice a week for 3 weeks, cells were washed twice with PBS, fixed in 95% ethanol for 30 min. And then added an appropriate amount of 0.1% Alizarin Red-Tris-Hcl (PH 8.3) staining for 30 min at 37°C following the ethanol being sucked. Observed and recorded the results under an inverted microscope. Detection of the activity and relative activity of alkaline phosphatase (ALP) was performed by enzyme-linked immunosorbent assay to detect the OD at 410 nm wavelength (the specific process not shown).

Migration: The P3 generation MSCs cell suspensions after digestion was prepared in the upper Transwell chamber with the cell density of 2.0×10^4 cells/cm^2 via automated cell counter. 5 ml DMEM medium was added in the upper chamber, a multi-polycarbonate film with 12 μm thickness was inserted in the middle of Transwell chamber and a 5 ml 10% FBS was joined in the lower chamber. The inferior vena of film was added with 5 ml DMEM, 5 mg blank microspheres and 5 mg drug-loaded microspheres in control group, blank microsphere group, and drug-loaded microspheres group, respectively. Each group included three parallels. After incubation in 37°C for 4 hours, the remnant cells in the upper Transwell chamber and multi-polycarbonate film were removed and the cells in lower chamber were fixed with 95% ethanol and stained by hematoxylin for 10 min. Randomly selected five horizons cell to count and record under the microscope.

The impact of local administration of drugs-load microspheres on the repair of bone deficits in SD rat

Clinically, the autologous or allogeneic bones are commonly grafted into the defect for the reconstruction of anatomical structure after debridement of osteoarticular tuberculosis. Bone defect model was established in this study for simulation and locally implanted with microspheres prepared to explore whether they affect the repairmen of bone tissue and the distribution of drugs.

Two millimeter length of tibia bone got from SD rat was inactivated by liquid nitrogen and then was replanted into the original defect to build bone defect model. Modeled animals were randomly divided into normal group, sham-operated group, blank microsphere group, and drug-loaded microspheres group. Three SD rats were randomly selected to be performed by X-ray, HE staining, bone alkaline phosphatase isozyme (B-ALP) and serum tartrate resistant acid phosphatase (TRAP-5b) for detection of bone tissue repair, hepatic and renal function to determine liver and kidney toxicity of the new microspheres, and local drug concentration of the surrounding bone and muscle tissue to estimate the distribution of drugs in vivo in 2th, 4th, 6th week from each group.

Statistical analysis

All data are presented as mean ± SD throughout this study. Statistical analysis of the experimental data with Student's t-test was performed by SPSS 19.0 software (SPSS, Inc., Chicago, IL, USA) and $P < 0.05$ is considered as significantly different.

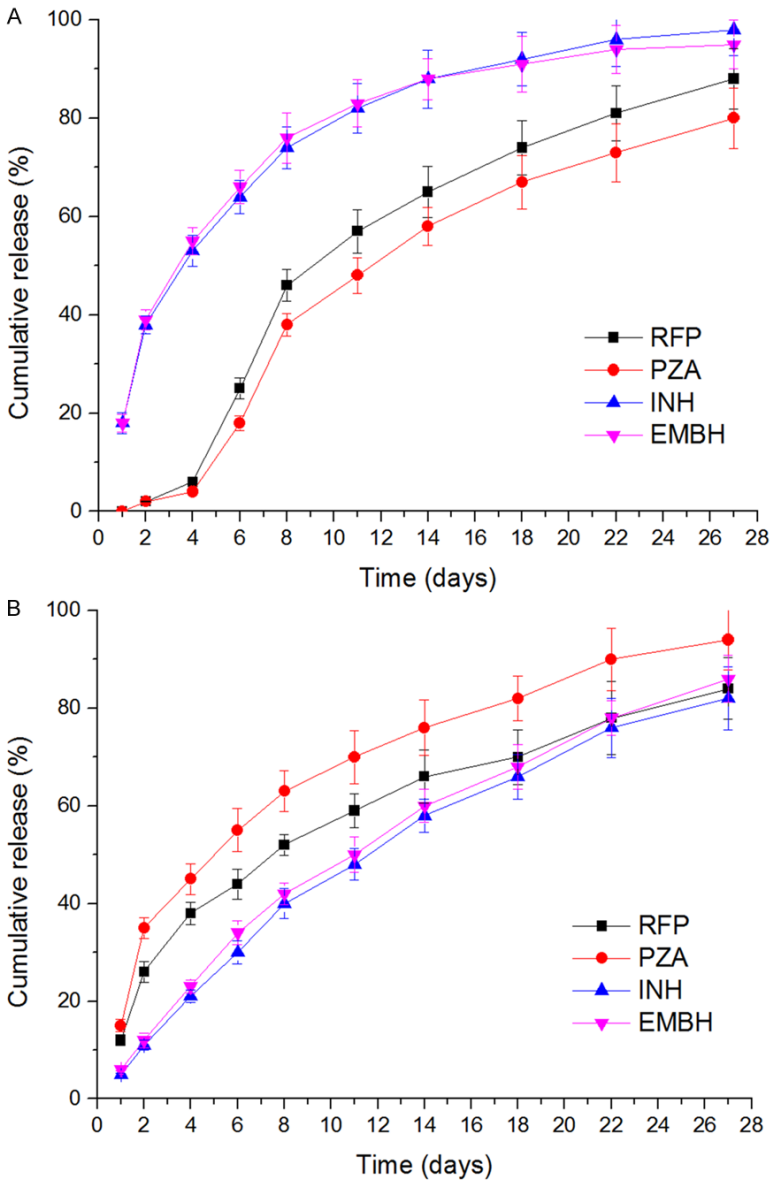

Figure 7. Percentage in vitro release profiles for microspheres in group B (A) and group C (B). RFP, rifampicin; PZA, pyrazinamide; INH, isoniazid; EMBH, ethambutol hydrochloride.

Results

Carrier concentration of PLLA and PLGA

Outcomes of carrier concentration under ordinary light microscope: Solute (PLLA and PLGA) concentration sequentially are 5%, 7.5%, 10%, 12.5% for preparing different microspheres by CEHDA. The microspheres fabricated in 7.5% and 10% concentrations were compared with the microspheres in 5% concentration and the uniformity structure of the microspheres was found better in 7.5% and 10% than 5% concentration. But when the solute concentration was increased to 12.5%, the coaxial needle presented with clogging and produced spinning phenomenon (**Figure 2**).

Outcomes of carrier concentration under CLSM: Coumarin-6 diffuse from the core to the shell in 5% concentration with a fuzzy boundary between core/shell, suggesting that there may be mixed PLLA and PLGA. However, coumarin-6 in 7.5% and 10% concentration showed no diffusion with the obvious boundaries between the core/shell (**Figure 3**).

Outcomes of carrier concentration under SEM: Microspheres in different carrier concentration demonstrated perfect dispersion and no significant adhesions (**Figure 4**).

Confirmation of drug-loaded core/shell structures

In this study, DCM and EA were used to dissolve PLLA and PLGA, respectively. As the dissolution of PLLA in EA is negligible, this polymer-solvent configuration is able to strongly reduce the diffusion between outer solution and inner solution at the tip of coaxial needle when going through the process of CEHDA. The existence of the core/shell structure within the drug-loaded microspheres fabricated from the carrier concentration of 10% and the core/shell flow rate ratio of 1.5 mL/h was confirmed by SEM and CLSM. The images of SEM and CLSM confirm that CEHDA can produce core/shell structured microspheres with distinct and tailorable distributions of cores and shells. In group B and C, the appearance color of microspheres

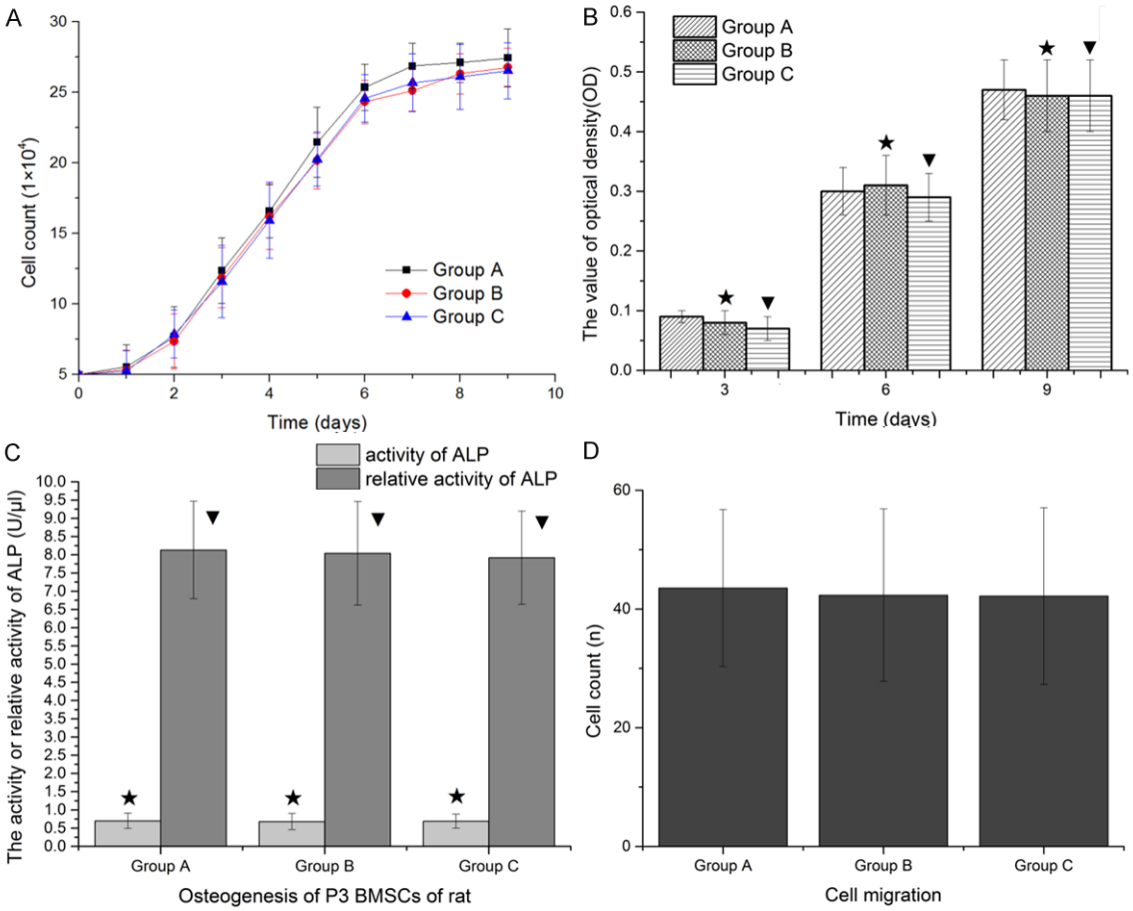

Figure 8. The impact of microspheres on biological behavior of BMSCs from SD rats. Group A, blank control group; Group B, blank microspheres group; Group C, drug-loaded microspheres group. A. Cell growth curve, there is no statistical significant difference between random two groups, $P > 0.05$; B. Cell viability, using MTT assay to record the optical density (OD) at 490 nm wavelength, Comparison between "▼" and "★" , $P > 0.05$; C. Osteogenesis evaluated by the activity and relative activity of alkaline phosphatase (ALP), comparison between "▼", $P > 0.05$, comparison between "★", $P > 0.05$; D. Migration, there is no statistical significant difference between random two groups, $P > 0.05$.

showed obvious differences when the hydrophobic RFP and PZA were wrapped in shell or core, and it demonstrates much darker color wrapped in shell than in core (**Figure 5**). There is no difference between groups (A, B and C) in microsphere size and the diameter of microspheres in group A, B and C was 18.07 ± 1.174 μm, 18.09 ± 0.80 μm, and 18.17 ± 0.903 μm, respectively (**Table 1**).

Application of core/shell microspheres in chemotherapy

Clinical reports suggest that INH/EMBH/RFP/PZA have additive effect on treating tuberculosis [8]. However, high initial concentration and/or a fast release are likely to pose serious toxicity to surrounding normal cells, so a high initial concentration of or a fast release is not recommended. In this study, core/shell structured microspheres with INH/EMBH (hydrophilic) entrapped in core and RFP/PZA (hydrophobic) encapsulated in shell (group C samples) were fabricated by CEHDA. Synchronously, microspheres with RFP/PZA (hydrophobic) entrapped in core and INH/EMBH (hydrophilic) encapsulated in shell (group B samples) were also designed for comparison (**Table 2**).

Encapsulation efficiency of drugs in microspheres

The encapsulation efficiencies of INH/EMBH/RFP/PZA in group B samples are about 39.2%, 46.4%, 85.2% and 83.7%, respectively. It is reasonable to notice high EE for RFP/PZA,

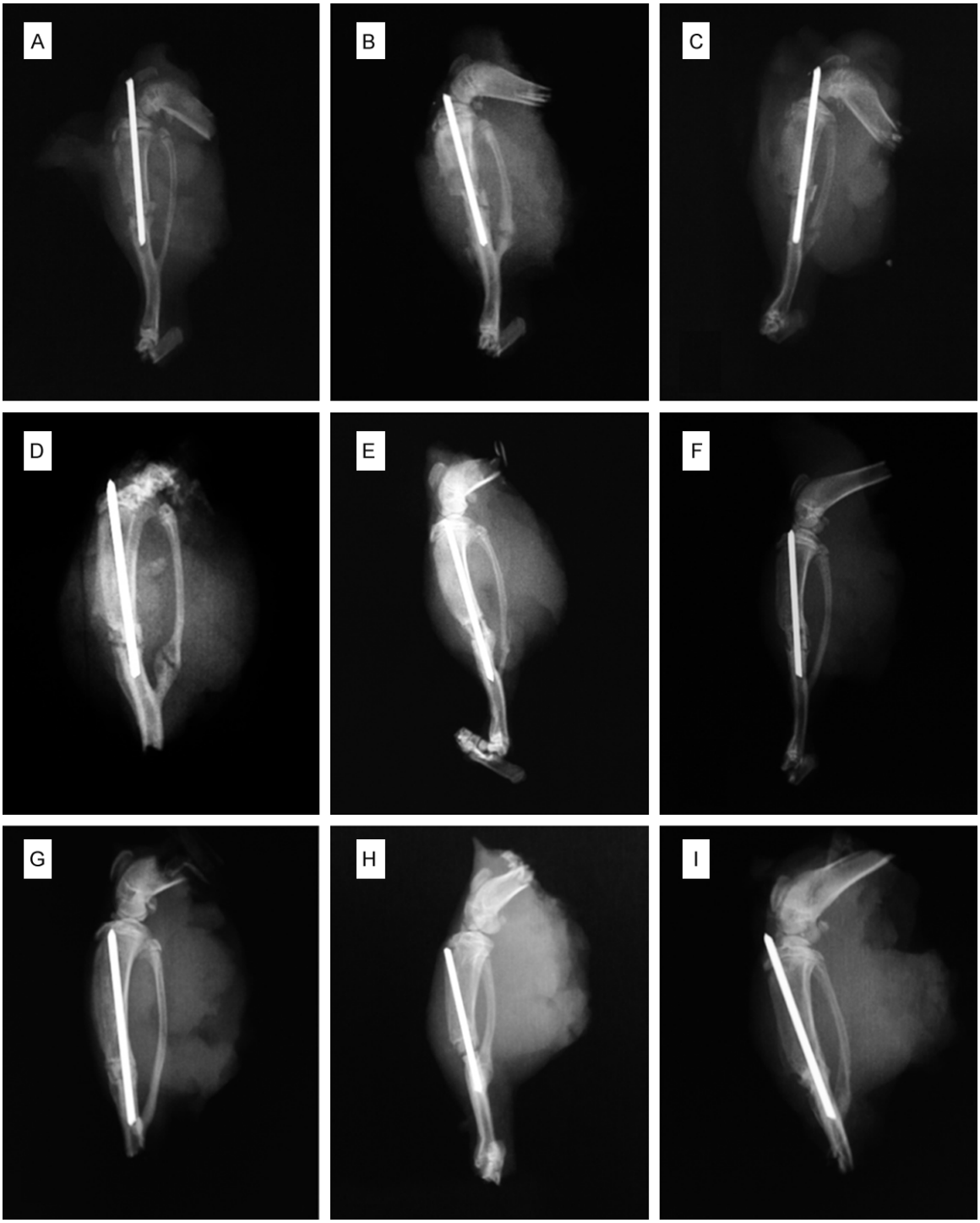

Figure 9. The impact of local administration microspheres on the repair of bone deficits in SD rat. (A-C, D-F and G-I) represent X-ray films at 2nd, 4th, and 6th week, respectively; (A, D, G), (B, E, H) and (C, F, I) represent sham-operated group, blank microspheres group and drugs-loaded group, respectively.

because it is loaded to the needle tip through the inner needle. This design reduces the possibility of diffusion of RFP/PZA into outer phase and gets wasted in the atomization process. In the case of INH/EMBH, its low EE is attributed to the jet instability caused by the outer solution (mixture of EA, ethanol and water). In group C samples, the EE of drugs are significantly

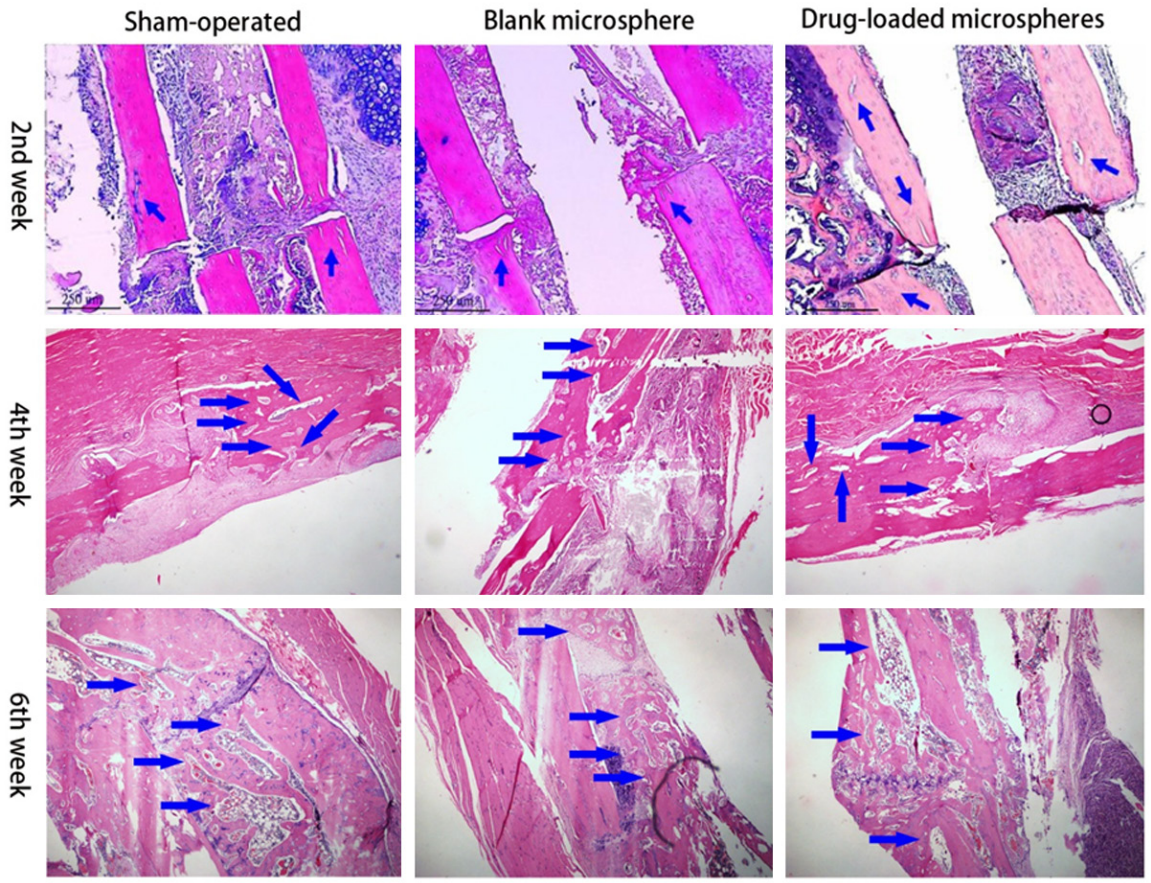

Figure 10. HE staining of bone tissue. The arrow indicates bone formation.

different. Compared with group B samples, lower EE of RFP/PZA was achieved, that is, 65.4%/60.1%. On the other hand, a significantly higher EE of INH/EMBH was obtained in group C samples, that is, 90.1%/91.3%. From the observations, it can be concluded that in all the samples higher EE is achieved for the drug loaded in the core as compared with the drug encapsulated in the shell. However, in the interest of overall EE, group C samples are advantageous over group B samples, because the EE of INH/EMBH is much higher in group C samples, whereas the EE of RFP/PZA is only slightly compromised (**Figure 6**).

In vitro release of drugs from microspheres

Because of totally different distributions of drugs in microspheres, two groups of samples demonstrate variable release profiles. Group B sample presents a significant initial burst of INH/EMBH (the release of INH and EMBH was almost similar) in which more than 50% of INH/EMBH is released out within the first 4 days of incubation. The release in the following days is more or less linear until day 28 when 90% of the INH/EMBH is released (**Figure 7A**). In contrast, the initial burst of RFP/PZA is minimal, only about 5% is released in the beginning 4 days. Then, 80% of the RFP and 70% of the PZA (the release of RFP and PZA was almost parallel) loaded is released linearly after 28 days (**Figure 7B**). Similar release results were reported by Nie at al [10, 11]. In the work done by Eckardstein et al. [12], the authors investigated the release of paclitaxel and suramin, which shares similar hydrophilic property with RFP/PZA and INH/EMBH, respectively. Form the release profiles of four drugs, it can be concluded that group B samples display a parallel release pattern of two drugs over the first 4 days, but show a sequential release if considered in the frame of 30 days.

Compared with group B samples, the release of four drugs from group C samples is relatively

Table 3. Hepatic and renal function, B-ALP and TRAP-5b

Index	Time (weeks)	Group A	Group B	Group C	Group C
ALT (U/L)	2	21.5 ± 6.5	23.2 ± 5.4	22.9 ± 6.3	24.2 ± 5.9
	4	23.4 ± 5.3	21.2 ± 6.7	21.9 ± 5.4	23.9 ± 4.6
	6	26.4 ± 4.8	22.3 ± 5.8	23.9 ± 6.1	24.2 ± 6.2
AST (U/L)	2	73.3 ± 11.3	79.7 ± 13.4	78.8 ± 15.1	79.2 ± 14.2
	4	75.5 ± 12.2	77.7 ± 13.5	75.1 ± 16.7	75.6 ± 13.6
	6	76.4 ± 14.2	74.7 ± 13.2	75.6 ± 14.5	79.9 ± 13.9
BUN (nmol/L)	2	6.9 ± 2.1	7.7 ± 3.2	7.4 ± 2.6	8.2 ± 1.9
	4	7.7 ± 2.7	7.8 ± 2.9	7.7 ± 3.2	8.9 ± 3.1
	6	7.5 ± 3.1	6.9 ± 2.4	7.6 ± 2.3	7.3 ± 3.6
Cr (μmol/L)	2	48.4 ± 9.8	47.4 ± 7.6	51.5 ± 8.7	49.2 ± 9.7
	4	54.8 ± 8.5	57.8 ± 8.4	49.9 ± 7.9	55.3 ± 8.7
	6	53.9 ± 9.1	58.6 ± 8.7	53.9 ± 9.7	57.2 ± 8.6
B-ALP (U/L)	2	112.9 ± 13.6	198.5 ± 34.5	190.4 ± 42.5	197.2 ± 42.8
	4	78.4 ± 12.7	154.5 ± 45.3	156.4 ± 35.6	160.7 ± 36.8
	6	55.3 ± 14.5	135.6 ± 36.2	125.9 ± 37.2	136.4 ± 35.7
TRAP-5b (U/L)	2	3.62 ± 0.21	5.22 ± 0.31	4.83 ± 0.37	5.16 ± 0.41
	4	4.15 ± 0.33	5.71 ± 0.43	5.54 ± 0.32	5.45 ± 0.38
	6	3.26 ± 0.29	4.89 ± 0.38	5.76 ± 0.35	5.53 ± 0.42

Note: Group A, B, C and D represents normal group, sham-operated group, blank microsphere group, and drug-loaded microspheres group, respectively. ALT (alanine transaminase) and AST (aspartate transaminase) are representative of hepatic function; BUN (blood urea nitrogen) and Cr (creatinine) are representative of renal function; B-ALP isozyme (bone alkaline phosphatase) and TRAP-5b (tartrate resistant acid phosphatase) for detection of bone tissue repair.

straightforward. They released about 40% of RFP/PZA and 20% of INH/EMBH over the first 4 days, and around 90% of PZA and 80% of RFP/INH/EMBH are released after 28 days (**Figure 7B**). The release profiles of four drugs are well coupled, although the release rate of PZA is slightly higher than RFP/INH/EMBH all the way. Different to the release pattern of group B samples, this pattern can be classified as a parallel release of four drugs.

The impact of drug-loaded microspheres on biological behavior of BMSCs from SD rats

Cell growth: Graphics of three groups showed a typical S-shaped curve, almost perfect correspondence. Number of cells in group A was slightly higher than that in group B and C from the fourth day of the beginning but with no statistical significance ($P > 0.05$). Cell growth in group B and C was basically consistent, as shown in **Figure 8A**.

Cell viability: MTT assay showed: OD value of the group B was slightly lower than group A, statistical analysis showed no significant difference ($P > 0.05$), indicating blank microspheres had no effect on the activity of rat BMSCs; OD value of group C was slightly lower than group A, no significant difference in the statistical analysis ($P > 0.05$), noting drug-loaded microspheres had no effect on the activity of rat BMSCs; comparison of OD values between group B and C showed no difference with statistical analysis $P < 0.05$, demonstrating the four first-line ant-TB drugs released from microspheres had no effect on the activity of rat BMSCs (**Figure 8B**).

Osteogenesis: Randomly selected several field to observe the osteogenesis. Blue represents for ALP staining and red for alizarin red staining. No visible difference between groups was observed with the light microscope. ALP activity reflects the comprehensively osteoinductivity, but the relative activity of ALP reflects the degree of osteogenic differentiation of rat BMSCs. The results showing the activity of ALP and relative activity of ALP between the 3 groups was not statistically significant ($P > 0.05$), indicating blank microspheres and drug-loaded microspheres had no effect on osteogenesis of P3 BMSCs of rat (**Figure 8C**).

Migration: All cells in each group were starved for 12 hours before experiment. Some cells

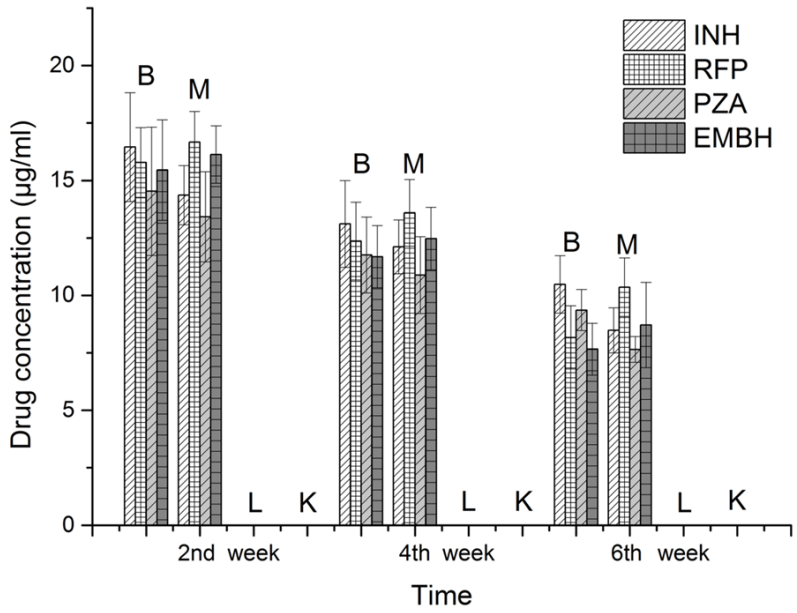

Figure 11. Distributions of drugs. B, surrounding bone tissue; M, surrounding muscle tissue; L, liver tissue; K, kidney tissue, the focal bone and muscle tissue manifest high drugs concentration and liver and kidney tissue have not be founded drug accumulation.

were founded with electron microscope on back of the film migrating from the upper Transwell chamber via membrane pores. Randomly selected five horizons, counted cell, and repeated three times (**Figure 8D**).

The impact of local administration of drugs-load microspheres on the repair of bone deficits in SD rat

The repair of bone tissue: Similarly to the sham-operated group, X-ray examination of blank microspheres group and drugs-loaded group showed no bone nonunion or delayed healing (**Figure 9**). The HE staining in the tissue sections of bone stump: appeared periosteal proliferation in the 2nd week; emerged new bone in bone defect in the 4th week; and existed obvious bone connection in lesion in the 6th week (**Figure 10**). Animals underwent surgical intervention were harvested significantly higher B-ALP, TRAP-5b than in normal animals ($P < 0.05$) and the modeling animals in each group showed no significant difference at each time point ($P > 0.05$) (**Table 3**).

Liver and kidney toxicity: Compared with the normal animals group, sham-operated, blank microsphere group and loaded microspheres animals showed no obvious elevating in parameters of hepatic and renal function ($P > 0.05$) (**Table 3**).

Drug distribution: Any ant-TB drug was not detected in liver and kidney tissue. Four kinds of ant-TB drugs within the local bone and muscle tissue could be detected and the local drug concentration of each drug was higher than the minimal inhibitory concentration (MIC) at the 2nd, 4th, 6th week ($P < 0.05$) (**Figure 11**).

Discussion

Core/shell structured microspheres as a novel drug delivery system, via coaxial electrohydrodynamic atomization (CEHDA), wrap multi-drug into the two separate compartments to achieve the purpose of controlling release time and ensuring drug release time consistent with therapeutic window to achieve the best therapeutic effect, which was called 'programmed release' [13, 14]. Currently, the clinically routine four first-line ant-TB drugs demonstrate different physical and chemical properties, and the combined administration can effectively avoid the formation of drug-resistant tuberculosis [15]. At present, the research on the controlled release of ant-TB drugs is merely confined to the sustained release of one or two drugs embedded in the carrier materials, which only succeed in extending release time of the drugs [5].

The methods of preparing core/shell structured microspheres include water emulsification [16-18] and CEHDA [10, 11, 14, 19]. Loscertales et al [20] elaborated the feasibility in applying CEHDA technology in theory and confirmed that two mutually incompatible solvent could form a stable 'Taylor cone' jet through the coaxial needle in a high voltage electric field. The two principles of fabrication of core/shell structure microspheres are the same and both based on differences in solubility of the solute in different solvents to form the core/shell structure of microspheres. However, there were also reports in the literature demonstrating that DCM, as a

solvent of PLLA and PLGA, could be made into the distinct core/shell structured microspheres by CEHDA equipment. Thus CDHEA device significantly reduced requirements for solvent.

With the increase of carrier concentration, the uniformity of microspheres size was gradually improved, the shell and core structure was progressively densified, and smoothness of the microspheres surface under the electron microscope and the core with coumarin-6 stained under the CLSM detection increased significantly [10]. In present study, when the carrier concentration exceeds a certain level, the spinning phenomenon appears, which was similar to some literatures [21-24] reported that when the carrier concentration of material PLGA and PLLA up to 30%, some coaxial wire can be prepared using the same preparation parameters. Therefore, the carrier concentration is the basis for the preparation of the core/shell structure of the microspheres. In this study, we selected the carrier concentration of 10% as the concentration of fabricating core/shell structure microsphere.

The hydrophobic RFP/PZA and hydrophilic INH/EMBH drugs were divided into two groups to ensure system stability in the inner and outer fluid according to the properties of the drugs (**Table 2**). The hydrophilic INH/EMBH drugs was dissolved in deionized water (DI) and then mixed with carrier material solution (CMS) by emulsification, forming a stable suspension (DI/CMS < 1/20), which significantly reduce the impact on the stability of inner and outer liquid system and finally ensure the stability of drug-loaded microspheres [10, 14, 16].

The identical ant-TB drugs packaged in the core or shell, but differ significantly in the encapsulation efficiency (EE) (**Figure 6**), which means the EE of core was obviously higher than the EE of shell, consistent with the results reported by Nie at al [11, 12]. The difference may be attributed to the following reasons: 1) the presence of differences in physical and chemical properties of the drugs will lead the slow release of hydrophobic drugs and rapid release of hydrophilic; 2) the carrier materials (PLLA and PLGA) can delay the release of drugs and the drugs in the core embedded in double wrapping of carrier materials with no drug aggregation in microsphere surface effectively avoid shortly explosive release at the early stage [19, 25] (**Figure 7A**); 3) the drugs embedded in the shell are in more contact with the outside in the process of collection and freeze-drying, so the EE was significantly lower than the core's; 4) the release of hydrophilic drug was significantly faster than the release of hydrophobic drug, but confined to the shell of PLGA, thereby multi-drug could achieve the purpose of synchronous release (**Figure 7B**). However, in order to avoid the formation of drug-resistant TB strains, multi ant-TB drugs are required to synchronously achieve the maximum peak release and continue maintaining the more effectively bactericidal concentration in the treatment of tuberculosis. Moreover, in present study, cell culture experiments and animal experiments have been carried out to evaluate the biological safety of drug-loaded microspheres in cell growth, cell viability, osteogenesis and migration of BMSCs in vitro and the repairmen of bone tissue of SD rat and the distribution of drugs in vivo.

Conclusion

In short, the work can prepare the core/shell structure microsphere of four first-line anti-tuberculosis drugs via CEHDA. When the concentration of carrier materials (PLLA and PLGA) reaches 10%, the distinct, uniform and stable core/shell structure of microspheres would be harvested. The microspheres with hydrophilic INH/EMBH embedded in core and hydrophobic RFP/PZA buried in shell can achieve the purpose of synchronous release. Furthermore, cell and animal experiments have demonstrated the drug-loaded core/shell structured microspheres have no effect on normal physiological activities of surrounding cells of BMSCs in vitro and the bone fusion in a bone deficits model in SD rat. These findings present the advantages and possible application of this kind of multi-drug release system in treating skeletal tuberculosis. Moreover, the characteristic sequential release of multi-drugs can be controlled and adjusted based on treatment need and used in treating other disorders.

Acknowledgements

This publication was funded by the National Natural Science Foundation of China (81171736), and Provincial Science & Technology department of Hunan, China (2014TZ2018; 2014GK3161).

Disclosure of conflict of interest

None.

Address correspondence to: Xiyang Wang, Department of Spine Surgery, The Xiangya Hospital of Central South University, 87# Xiangya Road, Changsha, Hunan 410008, People's Republic of China. Tel: +8613607317009; E-mail: 26211323-71@qq.com; Hemin Nie, Department of Biomedical Engineering, College of Biology, Hunan University, Changsha 410082, People's Republic of China. Tel: +8615211032998; E-mail: qtrbrs@163.com

References

[1] Dye C and Williams BG. The population dynamics and control of tuberculosis. Science 2010; 328: 856-861.

[2] Chen M, Gan H and Remold HG. A mechanism of virulence: virulent Mycobacterium tuberculosis strain H37Rv, but not attenuated H37Ra, causes significant mitochondrial inner membrane disruption in macrophages leading to necrosis. J Immunol 2006; 176: 3707-3716.

[3] Nagashima H, Yamane K, Nishi T, Nanjo Y and Teshima R. Recent trends in spinal infections: retrospective analysis of patients treated during the past 50 years. Int Orthop 2010; 34: 395-399.

[4] WHO global tuberculosis control report 2010. Summary. Cent Eur J Public Health 2010; 18: 237.

[5] Xu W, Wei X, Wei K, Cao X and Zhong S. A mesoporous silicon/poly-(dl-lactic-co-glycolic) acid microsphere for long time anti-tuberculosis drug delivery. Int J Pharm 2014; 476: 116-123.

[6] Zumla A, Nahid P and Cole ST. Advances in the development of new tuberculosis drugs and treatment regimens. Nat Rev Drug Discov 2013; 12: 388-404.

[7] Saikia C, Hussain A, Ramteke A, Sharma HK and Maji TK. Carboxymethyl starch-chitosan-coated iron oxide magnetic nanoparticles for controlled delivery of isoniazid. J Microencapsul 2015; 32: 29-39.

[8] Kaur R, Garg T, Malik B, Gupta UD, Gupta P, Rath G and Goyal AK. Development and characterization of spray-dried porous nanoaggregates for pulmonary delivery of anti-tubercular drugs. Drug Deliv 2014; 1-6.

[9] Qi B, Ji QS, Hou GH, Li L, Cao XF and Wu J. Comparison of conventional and directional freezing for the cryopreservation of human umbilical vein endothelial cells. Int J Ophthalmol 2014; 7: 768-772.

[10] Nie H, Fu Y and Wang CH. Paclitaxel and suramin-loaded core/shell microspheres in the treatment of brain tumors. Biomaterials 2010; 31: 8732-8740.

[11] Nie H, Dong Z, Arifin DY, Hu Y and Wang CH. Core/shell microspheres via coaxial electrohydrodynamic atomization for sequential and parallel release of drugs. J Biomed Mater Res A 2010; 95: 709-716.

[12] Von Eckardstein KL, Patt S, Kratzel C, Kiwit JC and Reszka R. Local chemotherapy of F98 rat glioblastoma with paclitaxel and carboplatin embedded in liquid crystalline cubic phases. J Neurooncol 2005; 72: 209-215.

[13] Nie H, Lee LY, Tong H and Wang CH. PLGA/chitosan composites from a combination of spray drying and supercritical fluid foaming techniques: new carriers for DNA delivery. J Control Release 2008; 129: 207-214.

[14] Lei L, Wang S, Wu H, Ju W, Peng J, Qahtan AS, Chen C, Lu Y, Zhang X and Nie H. Optimization of release pattern of FGF-2 and BMP-2 for osteogenic differentiation of low-population density hMSCs. J Biomed Mater Res A 2015; 103: 252-261.

[15] Zeng H, Wang X, Pang X, Luo C, Zhang P, Peng W, Wu P and Xu Z. Posterior only versus combined posterior and anterior approaches in surgical management of lumbosacral tuberculosis with paraspinal abscess in adults. European Journal of Trauma and Emergency Surgery 2014; 40: 607-616.

[16] Fang Q, Cheng Q, Xu H and Xuan S. Monodisperse magnetic core/shell microspheres with Pd nanoparticles-incorporated-carbon shells. Dalton Trans 2014; 43: 2588-2595.

[17] Zhao H, Wu F, Cai Y, Chen Y, Wei L, Liu Z and Yuan W. Local antitumor effects of intratumoral delivery of rIL-2 loaded sustained-release dextran/PLGA-PLA core/shell microspheres. Int J Pharm 2013; 450: 235-240.

[18] Choi DH, Subbiah R, Kim IH, Han DK, Park K. Dual Growth Factor Delivery Using Biocompatible Core–Shell Microcapsules for Angiogenesis. Small 2013; 9: 3468-3476.

[19] Farook U, Stride E and Edirisinghe MJ. Preparation of suspensions of phospholipid-coated microbubbles by coaxial electrohydrodynamic atomization. J R Soc Interface 2009; 6: 271-277.

[20] Loscertales IG, Barrero A, Guerrero I, Cortijo R, Marquez M and Ganan-Calvo AM. Micro/nano encapsulation via electrified coaxial liquid jets. Science 2002; 295: 1695-1698.

[21] Hu J, Wang X, Ding B, Lin J, Yu J and Sun G. One-step electro-spinning/netting technique for controllably preparing polyurethane nanofiber/net. Macromol Rapid Commun 2011; 32: 1729-1734.

[22] Xu Q, Qin H, Yin Z, Hua J, Pack DW and Wang CH. Coaxial electrohydrodynamic atomization process for production of polymeric composite microspheres. Chem Eng Sci 2013; 104.

[23] Yuan W and Liu Z. Controlled-release and preserved bioactivity of proteins from (self-assembled) core-shell double-walled microspheres. Int J Nanomedicine 2012; 7: 257-270.
[24] Xiao CD, Shen XC and Tao L. Modified emulsion solvent evaporation method for fabricating core-shell microspheres. Int J Pharm 2013; 452: 227-232.
[25] Liu P. Stabilization of layer-by-layer engineered multilayered hollow microspheres. Adv Colloid Interface Sci 2014; 207: 178-188.